Carolyn Sebastian
Matthew Drexler
Laila Mostafavi
Natalie Rice

ME338: Final Report

Use of SKYRC GNSS Performance Analyzer

We used the SKYRC GNSS performance analyzer to measure the top speed. The top speed we got the car to go to was 18 km/hr. This was what we measured the top speed to be when the car was just going straight. However, this is likely not the actual top speed, as we could not get the car to drive in a straight line until the car no longer accelerated. Our car modifications were not done with the purpose of affecting the speed, so we believe the top speed increased as our skills controlling the car and steering got better.

Mass Properties

We measured the total mass using one of the digital scales provided in the kit. We assumed that this scale was correctly calibrated, after we tared it to zero with nothing on it, and that it was an accurate measurement. The initial total mass measured was 821.3 g. As such, using g = 9.81 m/s^2 and W = mg, we obtained the final weight: W = 8.057 N. Our changes added 255 g, which led to an increased mass of 1076.3 g, so we obtained the final weight: W = 10.6 N.

Center of gravity (x, y, z)

We defined the origin at the rear right tire contact patch. The center of this patch is considered (0,0,0). We assumed that the car is perfectly symmetrical and that the frame is centered. The measured weight distribution is listed in *Table 1* of the appendix and the major frame measurements are in *Table 2*.

X-direction of CG location (front to rear):

$x = \frac{W_{front}}{W_{total}} \times L$ = (510.1/1023.2) * 190 mm = 94.72 mm

Distance from front axle = 190 mm - 94.72 mm = **95.27 mm forward from rear axle**

Y-direction of CG location (left to right):

$y = \frac{W_{left}}{W_{total}} \times T$ = (522.7/1023.2) * 234.5 mm = 119.80 mm

Distance from the right wheels = **119.80 mm from right side**

Z-direction of CG location (height):

Tilt angle = 45 degrees

$$z = \frac{Wheel\ Base * Front\ Mass\ Change}{Total\ Mass * Tan(Angle)} = \frac{190(510.1 - 128.63)}{1023.2 \times tan(45)} = 70.84\ mm$$

Distance from ground = **70.84 mm**

Center of Gravity: **(95.27 mm, 119.80 mm, 70.84mm)**

Major Frame Measurements

Using calipers we made the measurements, listed in *Tables 2 and 4* in appendix, of the frame of the RC car.

Steering Geometry

Steering angles were measured using goniometers placed under the left and right front wheels, with the wheels turned fully to the right and left. One arm of each goniometer was aligned parallel to the vehicle body along the front and rear tire faces, while a ruler aligned the other arm with the front tire in its turned position. The turning radius was determined by marking the starting position of the inside tire along a horizontal reference line, driving the car slowly without slipping, and recording where the tire crossed the line. We repeated this five times. We assumed that the initial position of the wheel hub was aligned straight. In *Table 3* in the appendix we have recorded the turning radius for multiple trials.

Steering Angles for Different Positions:

Full Left Turn:	Full Right Turn:
Left Wheel (inner) = 24°	Left Wheel (outer) = 21°
Right Wheel (outer) = 20°	Right Wheel (inner) = 25°

Average Steering Radius: 6.07 mm

Ackermann Steering Geometry: Understanding this relation in simple terms, the inner wheel must turn at a great angle compared to the outer wheel: $cot(\delta_o) - cot(\delta_i) = \frac{W}{L}$

Example calculation: Turn Left

W = track width = 185.33mm

L = wheelbase = 190 mm

$\delta_{inner} = 24°$

$\delta_{outer} = ?$

Plugged into Ackermann Equation to get $\delta_{outer} = 17.25°$

The car does in fact use Ackermann steering geometry because the outer angle is less than the inner angle, which physically makes sense. The outer angle was slightly less than the one we measured, $17.25°$ < 20°.

Our car doesn't drive in a constant radius circle because real-world forces like tire slip and weight transfer, which deviates from what is mathematically correct as soon as speed is increased. Based on our measurements, we are experiencing understeer. Since our actual outer angle is wider than the ideal Ackermann angle, our front tires are "scrubbing" and fighting each other. This causes us to lose front-end grip first, making the car push wide in turns rather than holding a tight, consistent line.

It is also important to note that although the rear axle width was increased in the redesign, the steering geometry was not directly affected. Ackermann steering relationships depend primarily on the front track width and wheelbase, which define the geometric relationship between the inner and outer steering angles. Since these parameters and the front steering linkage were not modified, the fundamental steering geometry remains unchanged. However, the wider rear axle can still influence overall vehicle handling by improving rear stability and weight distribution, which may indirectly affect how the car responds during turning.

<u>Reverse Engineer the RC Car</u>

In this part, we deconstructed the modified car, the exploded view below, and measured the mass and dimensions of the inner parts. We recorded our measurements made using calipers in *Table 4*. We have included an image of the deconstructed car in *Figure 1* in the appendix.

<u>Gear train measurement</u>

Using calipers, we measured the diameter of each gear in the gear train. The gear train configuration is the same configuration used in the front and rear axles, so for simplicity, we calculated the gear ratio that drives the axle for simplicity, we only provided measurements from one configuration (they were essentially duplicated). In *Table 5* in the appendix we included the gear train measurements.

***The gear train is as follows: Gear 4 drives Gear 1, Gear 1 drives Gear 2, Gear 2 drives Gear 3*

UPDATED Gear Ratio

$$Gear\ Ratio\ = \frac{Driven\ Teeth}{Driver\ Teeth}$$

Stage 1: Gear 4 and Gear 1 $\rightarrow \frac{50}{10}\ =\ 5$

Stage 2: Gear 1 and Gear 2 $\rightarrow$ On the same shaft, same speed and torque, therefore 1:1

Stage 3: Gear 2 and Gear 3 $\rightarrow \frac{32}{13}\ =\ 2.4615$

$$Total\ Gear\ Ratio\ =\ 5\ \times\ 1\ \times\ 2.4615\ =\ 12.31$$

NEW Total Gear Ratio = 12.31**:1**

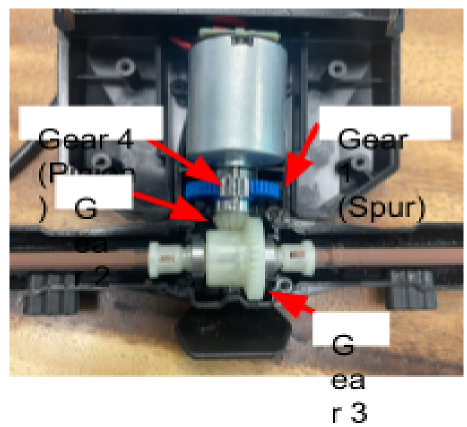

Figure 10. Gear configuration in rear axle with new gear.

<u>Battery Details</u>

The energy was calculated as the product of the listed voltage and capacity. The calculated energy and the listed one are equal, but in different units. The capacity of 1500 mAh means that the battery can discharge a current of 1500 mA for one hour.

When assuming a 20 min discharge time, the discharge rate was 3C. The current was calculated using the capacity over the discharge time. This value was divided by the capacity to obtain 3 hr^{-1}. Alternatively, this value can be calculated by finding the inverse of the discharge time in hours. We have included Listed battery specifications and calculated values in *Table 6* in the appendix.

<u>Suspension characterization</u>

Using calipers several measurements were made to characterize the vehicle's suspension. These measurements include: unloaded shock length, minimum, and loaded shock lengths. The difference between the minimum and maximum shock lengths is reported as the shock displacement. The unloaded shock length is measured without the load of the vehicle. The minimum shock length is measured by measuring the shocks while compressing the shocks removed from the car. The loaded shock length is measured with the car sitting on the ground; the shocks are loaded with the vehicle's weight. All measurements were made in mm, and are reported in *Table 8* in appendi*x.*

Because each loaded shock length is less than its unloaded length, we can deduce that the shocks, and therefore springs, are all pre-loaded. We have included data on shock lengths in *Table 7* in appendix.

Using the force gauge, we determined the stiffness of each spring. We used the gauge to measure the force required to compress the unloaded shocks to their minimum lengths. The ratio of the force over this change in displacement, measured with calipers, yielded the spring stiffness for each shock. These values are reported below in *Table 9* in N/m.

All four shocks are roughly the same. They have very similar measurements for both size, and stiffness. The variation in the recordings could be due to error in measurement, as recording the force proved challenging. Throughout this engineering design project, we will consider the differences between the shocks negligible.

Drive Motors and Servos (EE to ME conversion)

Using the provided FARC-280SA diagram (below), we determined several important values for our brushed motors. The maximum speed (RPM) that the motor is capable of is 14 000 RPM, and it occurs with no loading. At the maximum efficiency of 65%, the speed is 11600 RPM and the torque is 50g-cm. At the maximum power of 11 W, the motor's speed is about 7000 RPM and the torque delivered is 150 g-cm. Our RC car has similar specifications as it also utilizes a 280 motor.

Selected Races

After evaluating the performance of our RC car in Assignment 1 and analyzing the current components and their properties, we decided to redesign the vehicle to focus on the tractor pull and circuit race. We selected these events because we wanted to improve the traction of our vehicle and improve the steering. However, testing also revealed issues with traction and power delivery, particularly on uneven terrain. Improving traction and torque will benefit both the tractor pull, which requires high pulling force, and the circuit race requiring easier steering. To address these issues, several machine elements will be modified. The rear axle shaft will also be redesigned with a larger diameter and smoother transitions to increase torsional strength and reduce stress concentrations, while still interfacing with the existing drivetrain components with updated axle caps and wheel connections. Additional changes focus on improving traction. The tire rims will be redesigned and 3D printed with increased mass, increasing the normal force on the tires and therefore the maximum available traction. The rims will also accommodate a larger hex interface to match the modified shaft. Moreover, this task added serious weight to the vehicle, especially to the tires. This increase in weight made steering much easier, and allowed for competitive improvements in the circuit race. Finally, the gear ratio will be increased by either reducing the motor pinion gear size or increasing the driven gear size to increase torque at the wheels for the tractor pull event, though this will slightly reduce top speed. Together, these modifications improve the car's power delivery, traction, and drivetrain strength while remaining compatible with the existing components of the stock vehicle.

Improvements

Front Rim:

The original front tire rims were wrapped in wire until they reached a weight of 33g. This is 15g heavier than the original weight of the rims (18g), which was implemented to improve traction. These modifications are imaged in *Figure 1, element 1.* The improvements on traction are outlined in greater detail in the discussion of Weight Update. The weight of the front rims is included in *Table 4.*

Rear Rim Update:

The original rear tire rims were wrapped in wire until they reached a weight of 33g. This is 15g heavier than the original weight of the rims (18g), which was implemented to improve traction. The improvements on traction are outlined in greater detail in the discussion of Weight Update.

The rear rims were also designed with a 17.3mm hexagon insert to accommodate the modified 17mm wheel hex and 4mm screw.

The rear rims were also designed to have solid faces to improve with aerodynamics. Solid tires can slightly improve aerodynamics because their smoother surface creates less turbulence and allows air to flow more easily around the wheel. This can reduce both skin friction and flow separation, leading to a smaller wake behind the tire.

The rear tire rim is imaged in *Figure 1, element 2, and Figure 2.*

Weight Update:

An additional mass was intentionally added to the vehicle to improve performance in the tractor pull event. Increasing the total weight of the car increases the normal force acting on the tires, which directly increases the maximum frictional force available for traction. This allows the vehicle to transmit more torque to the ground without slipping, improving its pulling capability.

The added weight was placed near the center of the vehicle, close to the battery. This location was chosen to maintain overall balance rather than concentrating all the weight over the rear axle. By keeping the mass centrally located, the design avoids excessively unloading the front wheels, which could negatively impact steering control. This is especially important for the circuit race, where maintaining front-wheel contact and steering responsiveness is critical for navigating turns.

Placing the weight at the center also helps distribute loads more evenly across the chassis, reducing the likelihood of instability or uneven tire wear. While positioning the weight directly over the rear axle would maximize traction, it could lead to poor handling and increased understeer. The chosen placement provides a compromise, increasing traction enough to benefit the tractor pull while preserving stability and control during the circuit race.

However, the added mass still introduces trade-offs. The increased weight raises the vehicle's inertia, which reduces acceleration and makes it more difficult to change speed quickly. It also increases rolling resistance, which can reduce efficiency over multiple laps. Despite these drawbacks, the added weight is beneficial for the tractor pull, particularly on gravel surfaces. The increased normal force improves tire–ground interaction, allowing the tires to better grip the loose terrain and generate higher frictional forces. This reduces wheel slip and improves the vehicle's ability to effectively transfer torque to the ground. As a result, the added weight enhances traction on gravel while still maintaining acceptable performance in the circuit race.

The original mass of the car was 821.3g, which corresponds to 8.056953N. The modified rim design was printed with PLA and wrapped in wire until each rim reached a mass of 33g, which is 15g more per rim than the original vehicle. An additional 195g was added to the body of the car. The total additional mass added to the car was 255g, which corresponds to an additional weight force of 2.50155N. This is a 31% weight increase compared to the weight of the original car.

The normal force the car experiences is equal to the weight of the car, and the maximum available traction force is proportional to the normal force.

$$F_{traction} = \mu_k N \qquad \text{(Eq. 1)}$$

An increase in vehicle weight increases the normal force and therefore increases the maximum available traction. Under the same surface conditions, this modification is expected to increase the vehicle's maximum traction by approximately 31%.

The weight and mass distribution is outlined in *Table 1 and Table 4*. The added weight that was an addition change is depicted in *Figure 1* and labeled 7 in the appendix.

Gear Ratio Update:

To optimize an RC car for a tractor pull, the gear ratio should be adjusted to maximize torque at the wheels rather than speed. This is most effectively achieved by modifying the rear axle gear, either by increasing its size or pairing it with a smaller motor pinion. The rear wheels are usually responsible for pulling, so increasing their torque directly improves the car's ability to move heavy loads. A higher gear ratio slows wheel rotation but amplifies pulling force, which is ideal for tractor pull competitions. In a three-gear drivetrain, the intermediate gear primarily serves to transfer motion and reverse rotation, it usually does not significantly affect the overall gear ratio unless it is a compound gear with multiple sizes on the same shaft.

The original gear ratio was 10.34:1, which means that the axle turns once for every 10.34 turns of the motor. In order to increase the gear ratio, there are multiple changes we can make to the number of gear teeth, but we have decided to increase the number of teeth on gear 1 from 42 to 50. Modifying the spur gear gave us a gear ratio of 12.31 and about a 20% increase in torque. Torque is the rotational force that allows the wheels to push against the ground and pull a load, and it scales proportionally with the gear ratio. For every additional tooth added to the spur gear relative to the motor pinion, the mechanical advantage increases, meaning the motor's output force is multiplied by a greater factor before it reaches the wheels. In a tractor pull, this is critical because the car must overcome the increasing resistance of a weighted sled, requiring sustained, high pulling force rather than high rotational speed. While the tradeoff is a reduction in wheel RPM, meaning the car moves more slowly, this is an acceptable sacrifice in a tractor pull setting where raw pulling power is the primary objective.

The updated dimensions of the gear are shown in *Figure 7* along with the tolerances. Additionally, the calculations determining the gear ratio is shown in the Gear Train Measurement Section earlier in this report, with data from *Table 5*. The image of the updated gear is shown in *Figure 10*.

Rear Shaft Update:

For both the tractor pull and circuit race events, the rear shaft must be designed to balance high torque capacity with rotational efficiency and consistency. These events impose different performance demands on the drivetrain, requiring a design that is strong enough to handle heavy loading while still maintaining smooth and efficient motion over repeated laps. We have our design depicted in *Figure 3*.

For the tractor pull, the main requirement is the ability to transmit high torque without failure. This is addressed by increasing the diameter of the main shaft section, specifically Diameter 4, as stated in *Table 11*. We increased it from 4.3 mm to 4.8 mm to have a change of .5 mm which corresponds to a 11.6% increase. A larger diameter improves torsional strength and reduces the likelihood of excessive twisting or shear failure under heavy loads. The relationship governing this behavior is given by the torsion equation:

$$\tau = \frac{Tr}{J} \tag{Eq. 2}$$

The elements in this equation include τ, the shear stress on the shaft, r, radius of the shaft, and J, the polar monet of inertia of the shaft. J is represented by the equation below with d being diameter.

$$J = \frac{\pi d^4}{32} \tag{Eq. 3}$$

This shows that increasing the diameter significantly reduces shear stress, making the shaft more capable of handling the high torque demands of the tractor pull. This is especially important because failure in torsion is often sudden and catastrophic, meaning even a small reduction in stress greatly improves reliability. By increasing the diameter, the shaft not only resists immediate failure but also reduces angular deformation, which helps maintain consistent power transfer to the wheels under heavy loading conditions.

At the same time, the circuit race requires the shaft to operate efficiently over multiple laps, where excessive weight and rotational inertia can negatively impact acceleration and speed. A heavier shaft requires more energy to accelerate due to its increased moment of inertia, which can reduce responsiveness when exiting turns. Therefore, while the diameter is increased for strength, it is not oversized. The selected diameter provides sufficient torsional resistance while limiting added mass, ensuring the vehicle remains responsive and efficient during continuous motion. This balance is critical because overdesigning for strength would directly compromise speed performance.

Another key improvement that benefits both events is the reduction of stress concentrations. The shaft includes stepped diameter changes, which can create localized high-stress regions where cracks are more likely to initiate. Under repeated loading, these regions experience higher cyclic stresses, accelerating failure. Introducing smooth fillets reduces the stress concentration factor by allowing forces to flow more gradually through the geometry.

The important section at the shaft end, where the wheel assembly connects, is also modified to improve load distribution and stability. We increased diameter 1 by 1 mm as it changed from 4 mm to 5 mm to have a 25% increase in diameter. We also changed the length from 75.85 to 80.85 by increasing the length of the section consisting of diameter 1 from 5 mm to 10 mm. This increased engagement length at Diameter 1 spreads the transmitted forces over a larger contact area, reducing contact stresses and minimizing the risk of wear or deformation at the interface. This is particularly important for tractor pull, where large forces are transmitted through the connection. In the circuit race, this modification also improves alignment and reduces wobble. Even small misalignments can lead to vibrations, which increase energy losses, reduce traction consistency, and negatively impact handling over multiple laps.

Because these modifications alter the shaft geometry, associated components such as the axle cap and retaining screw must be updated to ensure proper fit and alignment. Maintaining precise alignment is critical because any looseness or mismatch can introduce backlash or uneven load distribution, both of which reduce drivetrain efficiency and increase wear over time. Additionally, since the rim is being redesigned, these changes can be integrated into the new wheel assembly without introducing additional constraints, allowing for a more cohesive and optimized system design.

Finally, all modifications are applied symmetrically to both rear shafts to ensure even torque distribution and balanced performance. Overall, the redesigned rear shaft successfully balances the high torque requirements of the tractor pull with the efficiency, durability, and consistency needed for the circuit race. These design choices are important because they address both immediate strength requirements and long-term performance, ensuring the shaft performs reliably under both extreme loading and repeated operational conditions.

Rear Wheel Hex Update:

The hex interface located between the wheel and axle is also modified to accommodate the updated shaft geometry. Because the shaft diameter at the connection point has changed, the original hex component would no longer provide a proper fit or secure torque transfer. As a result, the hex is resized to match the new shaft dimensions and maintain a tight, interference or properly constrained fit. This design is depicted in *Figure 4*.

This modification is important because the hex serves as the primary component responsible for transmitting torque from the shaft to the wheel. If the hex does not properly match the shaft, it can lead to slippage, uneven load distribution, or wear at the interface. These issues are especially critical in the tractor pull, where high torque loads could cause the hex to deform or strip, and in the circuit race, where repeated loading cycles could lead to gradual loosening or fatigue failure.

Additionally, ensuring a precise fit between the shaft and hex improves alignment of the wheel assembly. Poor alignment can introduce vibrations and energy losses, reducing overall drivetrain efficiency and negatively affecting vehicle performance over multiple laps. By updating the hex to match the new shaft dimensions, the design maintains reliable torque transfer, structural integrity, and consistent performance across both events.

Rear Wheel Screw Update:

The rear wheel retaining screw is also modified to accommodate the updated shaft dimensions and ensure proper assembly of the wheel system. Because the shaft diameter and engagement geometry have changed, the original screw would no longer provide the correct fit or sufficient clamping force. The updated screw is selected with the appropriate length and diameter to match the new shaft and hex interface.

This change is important because the screw plays a critical role in maintaining axial retention of the wheel assembly. If the screw is too short or undersized, it may not fully engage with the shaft, increasing the risk of loosening or failure under load. In the tractor pull, this could lead to the wheel detaching or slipping under high torque conditions. In the circuit race, repeated vibrations and cyclic loading could gradually loosen an improperly fitted screw, reducing stability and consistency over multiple laps.

Additionally, a properly sized screw ensures adequate clamping force, which helps maintain alignment between the shaft, hex, and wheel hub. This clamping force can be approximated by the relationship:

$$F = \frac{T}{Kd} \qquad \text{(Eq. 4)}$$

In this equation, F is the clamping force, T is the applied tightening torque, d is the nominal screw diameter, and K is a torque coefficient that accounts for friction in the threads and under the screw head.

This relationship shows that selecting the correct screw diameter and applying sufficient torque directly affects the clamping force generated at the interface. Higher clamping force increases friction between components, which prevents relative motion and reduces the risk of slipping under load.

By maintaining sufficient clamping force, the design minimizes wear and prevents energy losses due to micro-slipping at the interface. Updating the screw to match the new shaft geometry ensures secure fastening, reliable torque transmission, and consistent performance across both events. This screw is depicted in *Figure 1* labeled 6 in the appendix.

Wire Extension Update:

A tow line was attached to the rear of the vehicle for the tractor pull, and its length was intentionally chosen to provide a short running start. This design allows the car to build initial momentum before the full load is applied, rather than experiencing an immediate, high resistance force from rest.

This is important because starting from rest under a heavy load requires a large torque demand, which can lead to wheel slip or motor stalling. By allowing the vehicle to gain momentum first, the force is applied more gradually once the line becomes fully tensioned. This reduces shock loading on the drivetrain and allows the tires to maintain better traction with the ground.

As a result, the vehicle is able to pull more effectively during the race, especially on gravel where maintaining traction is critical. Overall, the tow line improves performance by enabling smoother force application, reducing energy losses from slipping, and increasing the likelihood of successfully completing the pull. We have depicted this extension in *Figure 1* labeled 8 in the appendix.

FEA Analysis

During testing, we noticed that the shaft would break when the wheels hit obstacles. We decided to investigate this breaking through FEA to better understand what was occurring, and how to prevent it. We broke two of our 3D shafts during testing, both in the same spot and after hitting them against obstacles (head on). We then determined that the failure occurred because of a bending moment that exceeded the material's capacity. The failure was through fracture at the point where the hollow shaft, accommodating the screw, met the solid part held by the bearings. This junction led to a really high stress concentration that caused a bending moment failure. Through FEA, we were able to quantify the stress and its location. Also, note that the safety factor used is SF = 1. We used this value as we wanted to understand the forces that would cause actual fracture and failure of the shaft.

Before conducting FE analysis, we tried to estimate the maximum bending moment that shaft could withstand. We utilized the following equation:

$$\sigma_{max} = \frac{M_{max} c}{I} \qquad \text{(Eq. 5)}$$

Substituting the following values for c and I, we can derive equation 6.

$$c = \frac{D_o}{2} \qquad \text{(Eq. 6)}$$

$$I = \frac{\pi}{64}\left(D_o^4 - D_i^4\right) \qquad \text{(Eq. 7)}$$

$$\sigma_{max} = \frac{32\, M_{max} D_o}{64\left(D_o^4 - D_i^4\right)} \qquad \text{(Eq. 8)}$$

Additionally, we consulted a PLA specification sheet to determine the bending strength to be about 85 MPa, we used this value as our maximum bending strength. Using this value and our shaft dimensions, we estimated that the maximum bending moment our car could withstand would be 0.371 Nm. When dividing this maximum by the distance from where the force acts to where the failure occurs, we determined that the maximum perpendicular force to the axle our custom shafts could withstand was 37 N.

Using the CAD shaft on Solidworks, and a custom material spec sheet uploaded for PLA, we generated *Figure 5* and *Figure 6* (Appendix). We fixed certain surfaces, and added a 30 N force perpendicular to the axle. The FEA analysis shows the shaft will fail at the junction and get crushed. This result supports what we experimentally determined in testing. At the failure junction, the maximum stress it could handle was 0.9 MPa, this number is about 10% the maximum bending strength we predicted using spec sheets. This maximum bending stress then corresponds to the maximum bending force load actually being closer to 3 N. This number is more reasonable than our simplification earlier as it considers the complex geometry of the shaft and how it concentrates stress at this junction.

This FE analysis is very enlightening as it informs us of how the geometry affects the strength of the part. It must be noted, however, that even this FE analysis is a simplification of all the forces and interactions of the components in the RC car. In this analysis we determined that our car's back wheels are sensitive to directly hitting obstacles, as these may cause bending stresses that result in the failure of the shaft.

Results

After implementing our changes, we saw improvement in our two races: circuit and tractor pull. In short, our best performances for each respectively, were 54 seconds for the circuit, and 680 grams. For the circuit race, we improved our time by 43 seconds, in the worst case. As for the tractor pull, we improved our pulling capacity by 80 grams. These serious improvements were due to several modifications to the RC car.

First, we added serious weight to the vehicle. We did so by changing the tire rims to 3D designed CAD ones, adding 15 grams each. Also, we attached a 200 gram weight to the center of the car. This added weight seriously improved the traction, as aforementioned, by 31%. This improved traction led to us being able to pull more weight in the tractor pull. Also, the added weight stabilized the car, which in turn made it much easier to steer. We believe that the difficulty in steering was the primary factor affecting our performance in the circuit race. This added weight improved our results.

Next, the other primary direction of modifications was improving the torque delivered to the wheels. We did so in two primary ways. First, we increased the gear ratio by utilizing a 3D printed CAD design. This increase in gear ratio slowed down the motor, and increased the torque delivered through the shaft to the wheels. Also, we designed new shafts and hexes to combine with our new wheel rims. The design of our shafts decreased stress concentrations by employing filleted edges. These new shafts were also thicker than the original ones. These changes in the shafts allowed them to transmit more torque into the wheels. Overall, the increased torque to the wheels gave them more power to pull weight, leading to an increased performance in the tractor pull.

Finally, with our improvement we were able to decrease the mean circuit race time to 56.33 seconds with a standard deviation of 2.08 seconds. The tractor pull average was 776.67 grams with a standard deviation of 5.77 grams. All trials are listed in *Table 9* of the appendix.

Through this project we learned a lot about project management, and how to implement design changes. We had a couple setbacks in this project, including a new battery that failed to work. Looking forward, we have a few new ideas we would implement had we had more time.

First, we would want to machine shafts out of a stronger material. Our FE analysis revealed that our shafts could only withstand very small perpendicular forces. This weakness limits our ability to compete in races like Baja. Ideally, we would machine our shaft out of a stronger material like metal, this would allow it to withstand larger perpendicular forces before shaft failure.

Also, another change we would implement is using a new battery that is compatible with our car. We bought an upgraded battery but it failed to work with the new car. Had we had more time, we would research out to integrate it into our RC car, or why it is not compatible.

Lastly, we would explore improving the tire material and tread design. While the added weight significantly increased traction, we believe that optimizing the tire composition could further enhance grip without relying solely on added mass. By experimenting with different rubber compounds or tread patterns, we could potentially achieve better performance in both the circuit and tractor pull events. This would allow us to maintain or even improve traction while reducing unnecessary weight, leading to a more efficient overall design.

Overall, this project demonstrated the importance of iterative design, testing, and analysis. Each modification we made had measurable effects on performance, reinforcing the value of data-driven decision-making in engineering. If given more time, we would continue refining our design with a focus on balancing strength, weight, and efficiency to further improve performance across all events. We have included images of the final car top view and auxiliary in the appendix as *Figure 8 and Figure 9*.

Appendix

Tables:

Table 1: Measured Weight Distribution

Load	**Weight (*g*)**	**Weight w/ Tilt (*g*)**
Front Left	259.8	62.75
Front Right	250.3	65.88
Back Left	262.9	446.13
Back Right	250.2	451.88
Front Axle Load	510.1	128.63
Rear Axle Load	513.1	898.0
Total Vehicle Weight:	1023.2	1023.2

Table 2: Major frame measurements in mm

Wheelbase (mm)	Axle length (mm)*	Front track width (mm)	Rear track width (mm)
190	192.17	234.5	252.6

* Note: we included the gear connector in the axle length measurement.

Table 3: Recorded Turning Radius for Multiple Trials

Trial	**Turning Radius (mm)**
1	6.11
2	5.94
3	5.87
4	6.28
5	6.15

Average Turning Radius = 6.07 mm

*Table 4: Modified Parts Dimensions**

Label	Part	Dimension measurements (mm)	Mass (g)	Weight (N)
1	Front Wheels	Inner rim diameter: 46.28 mm Outer rim diameter: 52.49 mm Tire diameter: 85.12 mm Wheel width: 50.17 mm	81 g	0.009807 N
2	Rear Wheels	Inner rim diameter: 17.33 mm Outer rim diameter: 57.73 mm Tire diameter: 85.12 mm Wheel width: 50.17 mm	81 g	0.009807 N
3	Gears	Measurements listed in section 6, below	1.5 g	.015 N
4	Half * Rear Axle	Length: 80.9 mm Diameter 1: 5 mm Diameter 2: 6.33 mm Diameter 3: 3.9 mm Diameter 4: 4.80 mm Diameter 5: 8.90 mm	1.4 g	.0147 N
5	Rear Wheel Hex	Outer Diameter: 17 mm Inner Diameter: 5.05 mm	1.4 g	0.0137 N

6	Rear Wheel Screw	M4-.7x30	3 g	.029 N
7	Added Weight	Length: 57.5 mm Height: 34.7 mm Width: 29.1 mm	195.6 g	1.918 N
8	Wire Extension	Length: 363.5 mm	5 g	.049 N

* Note: Tolerances of CAD Components included in drawings in appendix.
* Note: The full rear axle comprises two identical components. It is connected by a gear train.

Table 5: Gear train measurements

Gear Number	Diameter (mm)	Number of teeth
1	26.51	50
2	12.24	13
3	24.87	32
4, motor gear	7.10	10

Table 6: Listed battery specifications and calculated values:

Listed voltage (V)	Listed Capacity (mAh)	Listed Energy (Wh)	Calculated Energy (kJ)	Discharge Rate (C-value in hr^{-1})
7.4	1500	11.1	39.96	3

Table 7: Shock lengths

Shock	Unloaded shock length (mm)	Minimum shock length (mm)	Loaded shock length (mm)	Shock displacement (mm)
Front Left	63.33	51.90	58.80	6.90

Front Right	63.34	51.93	58.82	6.89
Rear Left	63.32	51.92	62.73	10.81
Read Right	63.33	51.90	62.70	10.80

Table 8: Spring stiffness for suspension

Shock	Force recorded on gauge (N)	Shock displacement (m)	Spring stiffness (N/m)
Front Left	5.82	0.01143	509.17
Front Right	5.87	0.01141	514.46
Rear Left	5.89	0.01140	516.67
Read Right	5.83	0.01143	510.06

Table 9: Final Results

	Trial 1	Trial 2	Trial 3
Circuit Race (s)	54	58	57
Tractor Pull (g)	780	770	780

Sources:

PLA Spec Sheet: https://www.iemai3d.com/wp-content/uploads/2021/03/PLA_TDS__EN.pdf

Equations derived from Machine Elements Book:

Juvinall, R. C., & Marshek, K. M. (2020). *Fundamentals of Machine Component Design* (7th ed.). John Wiley & Sons.

Figures:

Figure 1: Exploded labeled view of car components

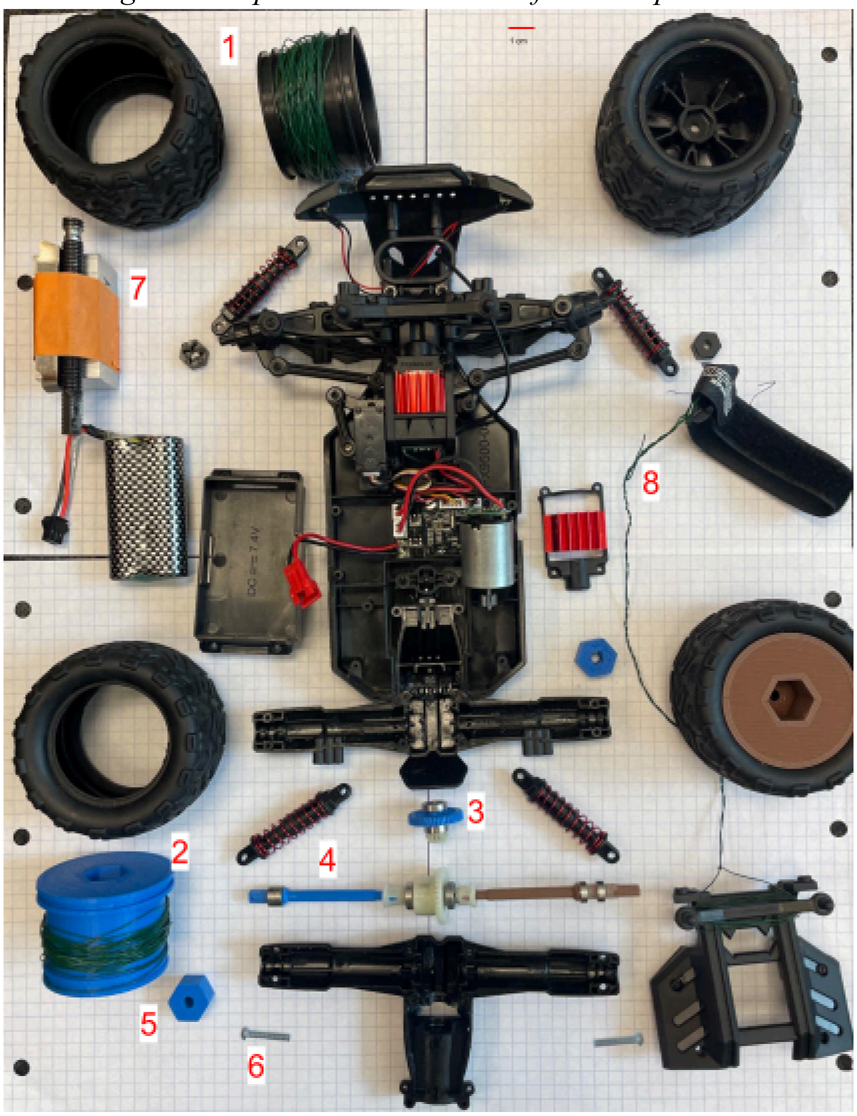

**Note: Label Numbers correspond with Table 4*

Figure 2: Drawing of Rear Rims with GD&T

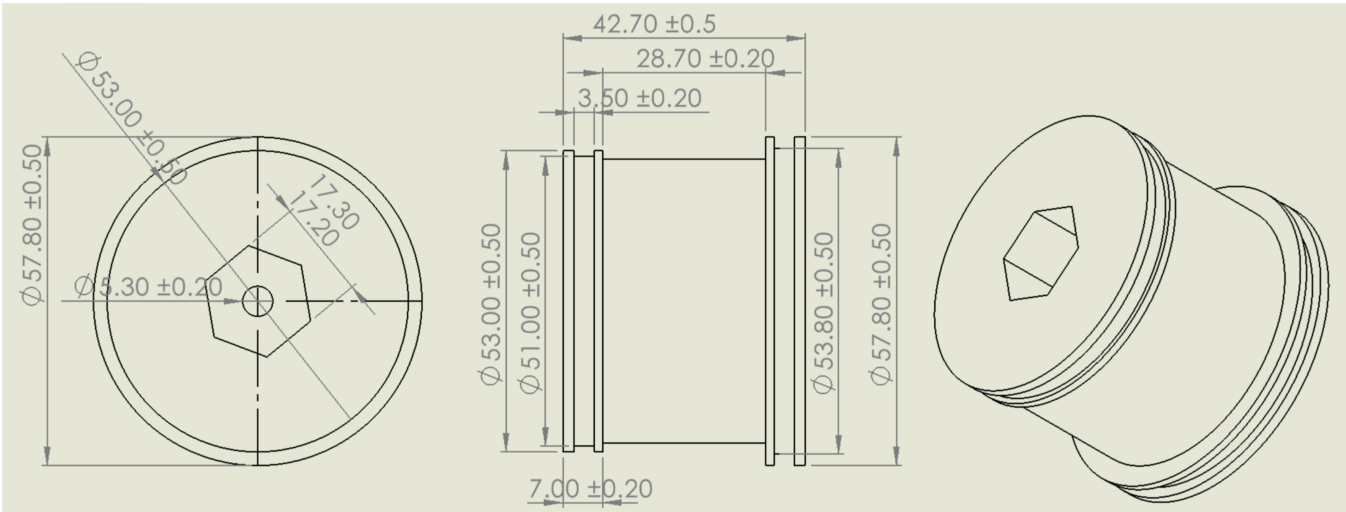

Note: All dimensions are in millimeters.

Figure 3: Drawing of Rear Axle with GD&T

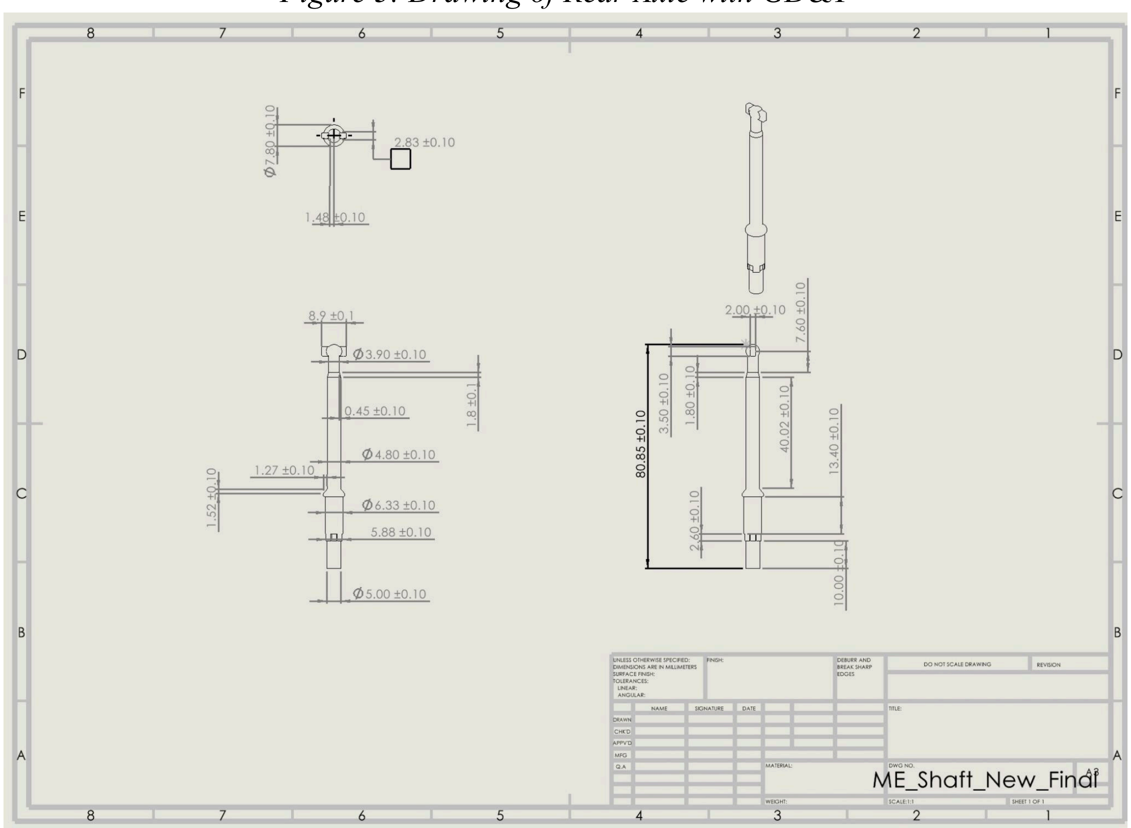

Note: All dimensions are in millimeters.

Figure 4: Drawing of Rear Wheel Hex with GD&T

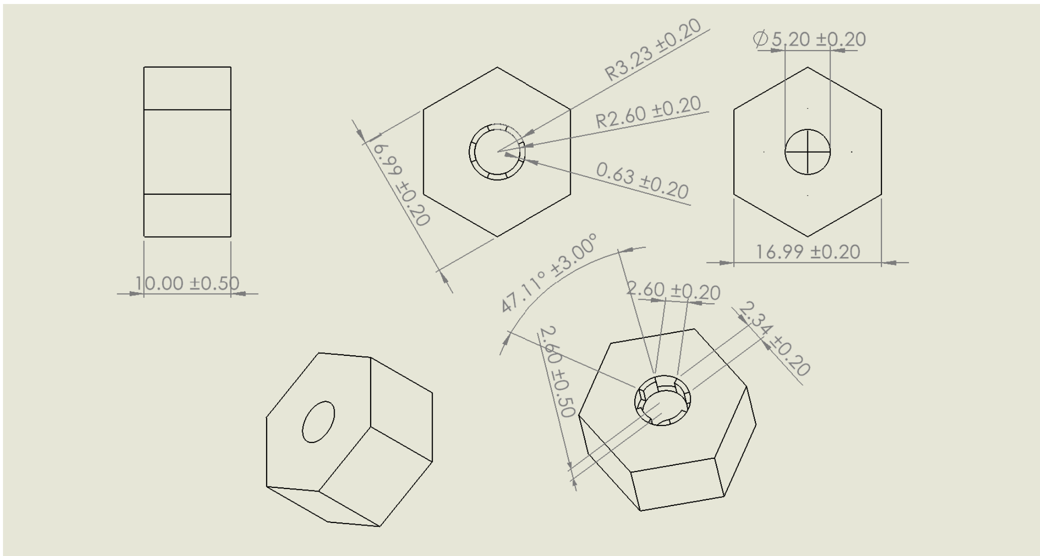

Note: All dimensions are in millimeters.

Figure 5: Shaft FEA Image 1

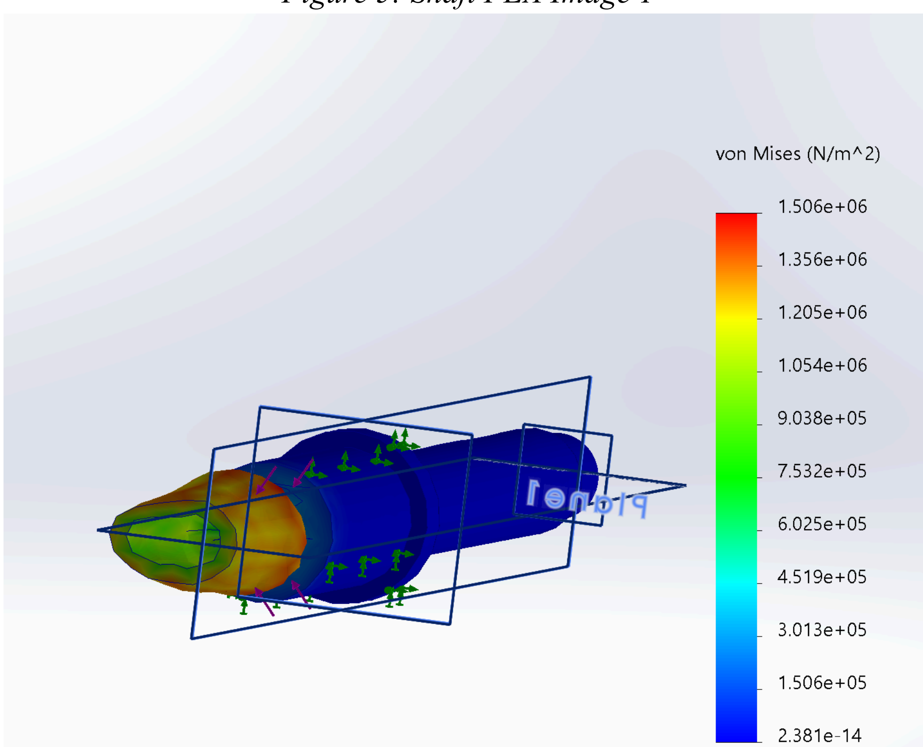

Figure 6: Shaft FEA Image 2

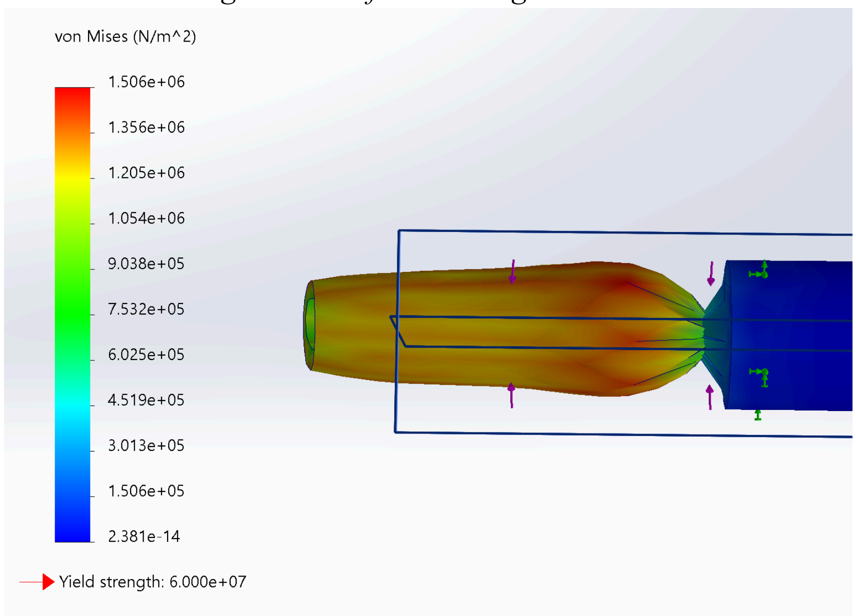

Figure 7: Spur Gear Dimensions with GD&T and Tolerances

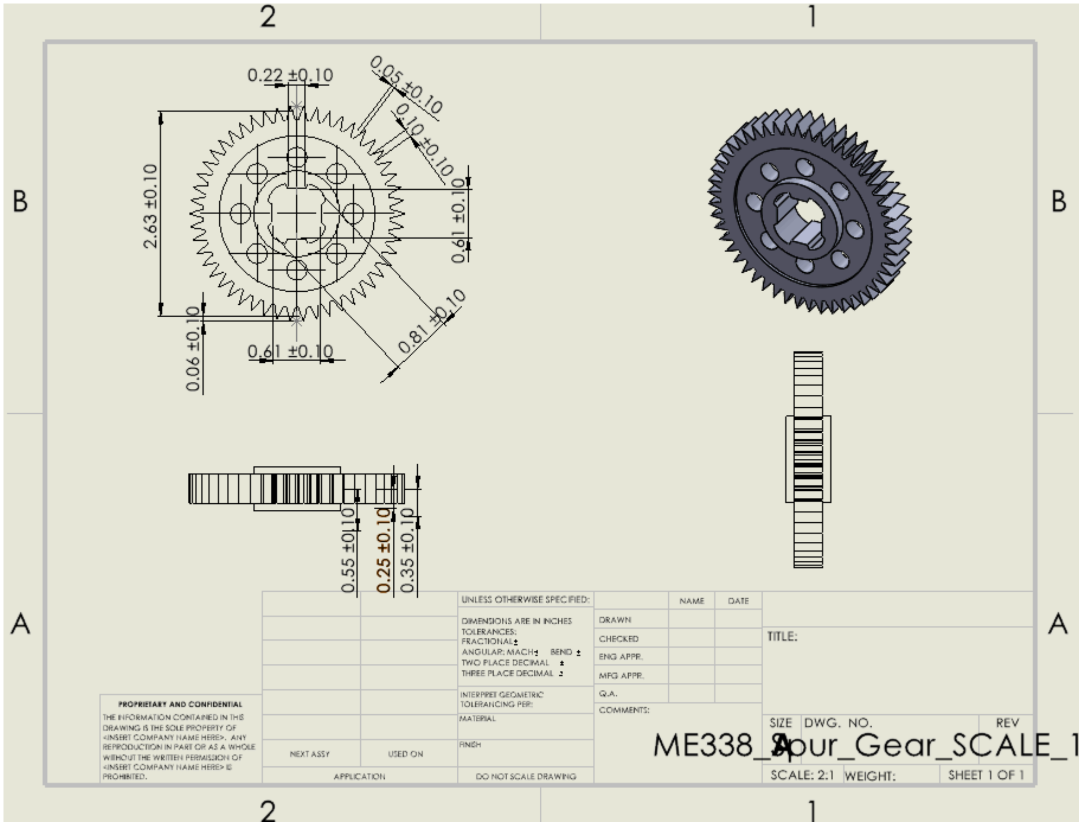

Note: Dimensions for spur gear are in centimeters.

Figure 8: Top View of Car

Figure 9: Auxiliary View of Car